


## Article

# A Novel Epoxy Resin-Based Composite with Zirconium and Boron Oxides: An Investigation of Photon Attenuation

Mohamed Elsafi <sup>1,\*</sup>, Nouf Almousa <sup>2</sup>, Fahad I. Almasoud <sup>3,4</sup>, Mansour Almurayshid <sup>3</sup> , Amjad R. Alyahyawi <sup>5,6</sup> and M. I. Sayyed <sup>7</sup>

<sup>1</sup> Physics Department, Faculty of Science, Alexandria University, Alexandria 21511, Egypt

<sup>2</sup> Department of Physics, College of Science, Princess Nourah bint Abdulrahman University, P.O. Box 84428, Riyadh 11671, Saudi Arabia

<sup>3</sup> Nuclear Science Research Institute, King Abdulaziz City for Science & Technology (KACST), P.O. Box 6086, Riyadh 11442, Saudi Arabia

<sup>4</sup> Department of Soil Sciences, College of Food and Agricultural Sciences, King Saud University, P.O. Box 2460, Riyadh 12372, Saudi Arabia

<sup>5</sup> Department of Diagnostic Radiology, College of Applied Medical Sciences, University of Ha'il, P.O. Box 2440, Ha'il 81451, Saudi Arabia

<sup>6</sup> Centre for Nuclear and Radiation Physics, Department of Physics, University of Surrey, Guildford GU2 7XH, UK

<sup>7</sup> Department of Physics, Faculty of Science, Isra University, Amman 11622, Jordan

\* Correspondence: m.elsafi.phy@alexu.edu.eg



**Citation:** Elsafi, M.; Almousa, N.; Almasoud, F.I.; Almurayshid, M.; Alyahyawi, A.R.; Sayyed, M.I. A Novel Epoxy Resin-Based Composite with Zirconium and Boron Oxides: An Investigation of Photon Attenuation. *Crystals* **2022**, *12*, 1370. <https://doi.org/10.3390/cryst12101370>

Academic Editor: Evgeniy N. Mokhov

Received: 6 September 2022

Accepted: 25 September 2022

Published: 27 September 2022

**Publisher's Note:** MDPI stays neutral with regard to jurisdictional claims in published maps and institutional affiliations.



**Copyright:** © 2022 by the authors. Licensee MDPI, Basel, Switzerland. This article is an open access article distributed under the terms and conditions of the Creative Commons Attribution (CC BY) license (<https://creativecommons.org/licenses/by/4.0/>).

**Abstract:** We have attempted to develop the gamma radiation shielding abilities of newly prepared epoxy composites by introducing ZrO<sub>2</sub>. The radiation shielding parameters are experimentally reported below. The experimental setup included an HPGe detector and different radioactive point sources which emitted photons with energies of 0.06, 0.662, 1.173, and 1.333 MeV. The gamma radiation shielding abilities of the epoxy composites were examined in the context of the linear attenuation coefficient (LAC), half-value layer (HVL), radiation absorption ratio, and other factors. The experimental and Phy-X results for the LAC were compared, and acceptable consistency was reported. The lowest LAC values were reported for EBZr-0 (free of ZrO<sub>2</sub>), and we found that the photon attenuation competence of the present epoxy improved as a result of increasing the ZrO<sub>2</sub> content. We compared the LAC values for the present epoxy composites with other samples, and we found that the prepared composites with 20% to 40% ZrO<sub>2</sub> had higher LAC values than epoxy with 30% Yahyali Stone. The HVL lengths of the epoxy composites reduced with the addition of ZrO<sub>2</sub> for the four selected energies, which confirmed that introducing ZrO<sub>2</sub> improves the radiation absorption abilities of epoxy composites. At 0.06 MeV, the HVL for the ZrO<sub>2</sub>-free epoxy was 2.60 cm, which fell to 0.23 cm after adding 40% ZrO<sub>2</sub>. The mean free path (MFP) for the prepared composites was less than 1 cm at 0.06 MeV (standard for EBZr-0), while it was 1.32 cm for EBZr-10. For the other energies, it was higher than 6 cm, and became higher than 10 cm at 1.333 MeV for all composites. The obtained results suggest that non-toxic, natural, and cheap epoxy composites with high ZrO<sub>2</sub> content have the potential to improve the gamma ray shielding competence of epoxy composites for low energy radiation applications.

**Keywords:** epoxy; ZrO<sub>2</sub>; gamma rays; shielding; radiation absorption ratio

## 1. Introduction

The demand for effective radiation shielding materials is increasing as more technologies begin to use radiation to function. Radiation is extensively used in the fields of medicine and agriculture, and in many others [1–3]. However, radiation can also cause immense harm to humans and the environment if they are exposed to the high energy photons for a long period of time. Three strategies are often used to minimize the potential

side effects that might occur when working with radiation: time, distance, and shielding. The first two principles relate to minimizing the time under exposure and maximizing the distance from the radiation source. In addition to these two principles, radiation shields are used to absorb high energy photons. These shields are placed between the radiation source and humans or the environment and are specifically designed to attenuate as much radiation as possible [4–7].

In addition to being effective at blocking radiation, depending on the desired application, these shields can be tailored to have different characteristics to make them as efficient as possible [8,9]. These characteristics vary from being lightweight to being thin, transparent, resistant to chemical and thermal exposure, able to block a wide range of photons, and more [10]. Concretes, for example, when combined with other additives, can be effective at blocking neutrons and gamma rays, and are widely used as a lining for X-ray rooms. However, concretes tend to develop cracks over time and lose their water content, so these properties must be considered and/or the concrete must be enhanced to improve these properties. Other materials such as polymers are being researched for their use in radiation shielding applications [11–13].

Epoxy resin, a type of polymer, contains many hydrogen atoms, which are highly effective at attenuating neutrons. In addition, epoxy composites have excellent mechanical properties, great chemical resistance and adhesive strength, and are suitable for harsh environments such as nuclear power plants [14–17]. By introducing additives with high atomic numbers, the shielding abilities of epoxy can be further improved. For instance, Chang, L. et al. [18] prepared epoxy composites filled with different weight percentages of tungsten and tested them against gamma rays. Their results showed a positive relationship between shielding ability and tungsten content in the epoxy, at the expense of the mechanical properties of the material. Additionally, Alduhaibat, M. et al. [19] tested  $\text{Al}_2\text{O}_3$ -epoxy and  $\text{Fe}_2\text{O}_3$ -epoxy at two different weight percentages each and found good results for some radiation shielding parameters.

To estimate the lifespan of epoxy-based composites, Saiyad M. and Devashrayee N. [20] irradiated several different materials with gamma radiation. Epoxy materials with lead and graphite were found to be the most effective at absorbing gamma radiation. A composite with vanadium slag, epoxy resin, and antimony-trioxide was prepared by Kavanoz, H. et al. [21] for radiation shielding applications as well as fireproofing. The composite had better shielding properties than concrete, but they were slightly less effective than those of lead. Another composite made of waste sawdust, waste PVC shavings, waste eggshells, vermiculite, and epoxy as a binder, produced by Sevinc, A. and Durgun M. [22], exhibited good attenuation abilities at the energies tested. Sahin, N. et al. [23] investigated an epoxy polymer matrix with Yahyali stone, a natural stone found in Turkey. The composite was found to be a low-cost, natural, and effective non-toxic radiation shield. Furthermore, the introduction of nanoparticles into epoxy composites has also been tested. Zhang, T. et al. [24] prepared  $\text{Bi}_2\text{O}_3$ - $\text{Ti}_3\text{C}_2\text{T}_x$  epoxy composites, and these samples were found to be effective at a wide range of energies. Like other heavy metal oxides such as lead, tungsten, and hafnium oxides, zirconium dioxide ( $\text{ZrO}_2$ ) has been proposed in the literature as an additive to low-density shielding material with the basic promise of enhancing the shielding competences. Shielding composites with additional  $\text{ZrO}_2$  content have shown greater attenuation performance compared with neat epoxy. Aside from their great radiation attenuation potential,  $\text{ZrO}_2$ -reinforced epoxy composites are arousing interest for their durability, low cost, low weight, and low toxicity, all of which make it an ideal alternative to heavy shielding materials in personal protective equipment.

In this work, non-toxic, natural, and cheap epoxy compounds with high  $\text{ZrO}_2$  content were prepared in order to study their radiation attenuation properties against different energies of photons. This study was performed by employing the typical narrow beam transmission geometry for the gamma radiation attenuation set up where the investigated photon energies were 0.06, 0.662, 1.173, and 1.333 MeV. The radiation shielding parameters were examined in the context of the LAC, MFP, and  $Z_{\text{eff}}$ . The major contribution of

the present study is our conclusion that the use of non-toxic, natural, and cheap epoxy composites enriched with high amounts of  $ZrO_2$  have the potential to enhance gamma ray shielding ability for low energy radiation applications.

## 2. Materials and Methods

### 2.1. Preparation

New composites based on epoxy resin and zirconium oxide in addition to a small percentage of boron oxide were prepared. “Generic” brand epoxy resin, in the form of a transparent liquid, was purchased from a local store. The two other oxides ( $ZrO_2$  and  $B_2O_3$ ) were purchased from El-Gamhoria Company in Egypt. These oxides were sieved using a sieve with 60  $\mu m$  hole diameters. These three components were mixed in the proportions displayed in Table 1 to get five different samples, which were prepared in the traditional mixing way, as shown in Figure 1.

**Table 1.** The compositions of the prepared samples.

Sample Code	Composition (wt %)			Density ( $g \cdot cm^{-3}$ )
	Epoxy	$B_2O_3$	$ZrO_2$	
PBT-0	85	15	0	1.282
PBT-10	75	15	10	1.402
PBT-20	65	15	20	1.548
PBT-30	55	15	30	1.727
PBT-40	45	15	40	1.953



**Figure 1.** The prepared samples used in this study.

### 2.2. Attenuation Measurements

Attenuation parameters were calculated experimentally using an HPGE detector and various radioactive sources. Geometric measurement was designed using the collimated beam technique, as shown in Figure 2. The source–sample distance was 15 cm, while the sample–detector distance was about 4 cm. The net count rate ( $N$ ) of the sample, and its absence ( $N_0$ ), were calculated in the same conditions with each emission of energy from the source using help Genie 2000 software. From the count rate values, the linear attenuation coefficient ( $LAC$ ) can be identified through the following equation [25–29].

$$LAC = \frac{-1}{x} \ln \frac{N}{N_0} \quad (1)$$

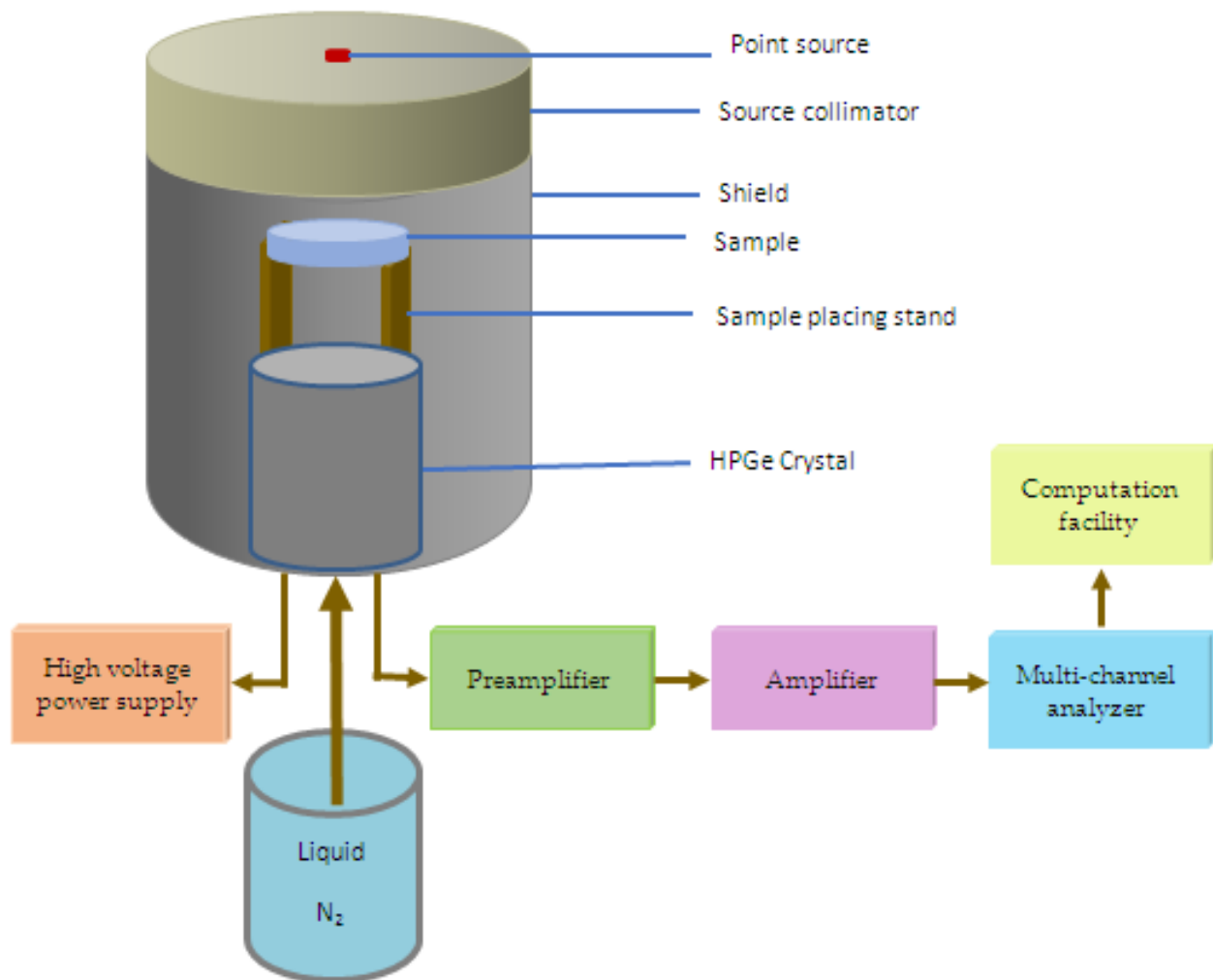


**Figure 2.** The arrangement of the experimental work.

Some of the shielding quantities for the epoxy resin samples reinforced with ZrO<sub>2</sub> and B<sub>2</sub>O<sub>3</sub> were calculated as described elsewhere [30–35].

### 3. Results

Using the experimental setup outlined in the previous section, we measured the intensities of the incident and transmitted radiation. This helped the authors to report the experimental linear attenuation coefficients (LACs) for the epoxy samples (EBZr-0 to EBZr-40). The LAC values were determined using Phy-X software (these were theoretical results for the LACs, and we aimed from these calculations to check the consistency between the measured and calculated LACs). According to the measured and Phy-X program calculations, the variation in the LACs for the EBZr-0 to EBZr-40 samples against four photon energies (0.060–1.333 MeV) is graphed in Figure 3. According to the data presented in the figure, small deviations between the measured and Phy-X values of 1.07–4.78% for EBZr-0, 0.28–2.11% for EBZr-10, 0.46–0.7% for EBZr-20, 1.74–4.69% for EBZr-30, and 0.66–3.81% for EBZr-40 were reported. These deviations indicate high accuracy in the experimental LAC values for the prepared epoxy samples (EBZr-0 to EBZr-40). Accordingly, we used these experimental LAC values to study other shielding parameters for our prepared epoxy samples.

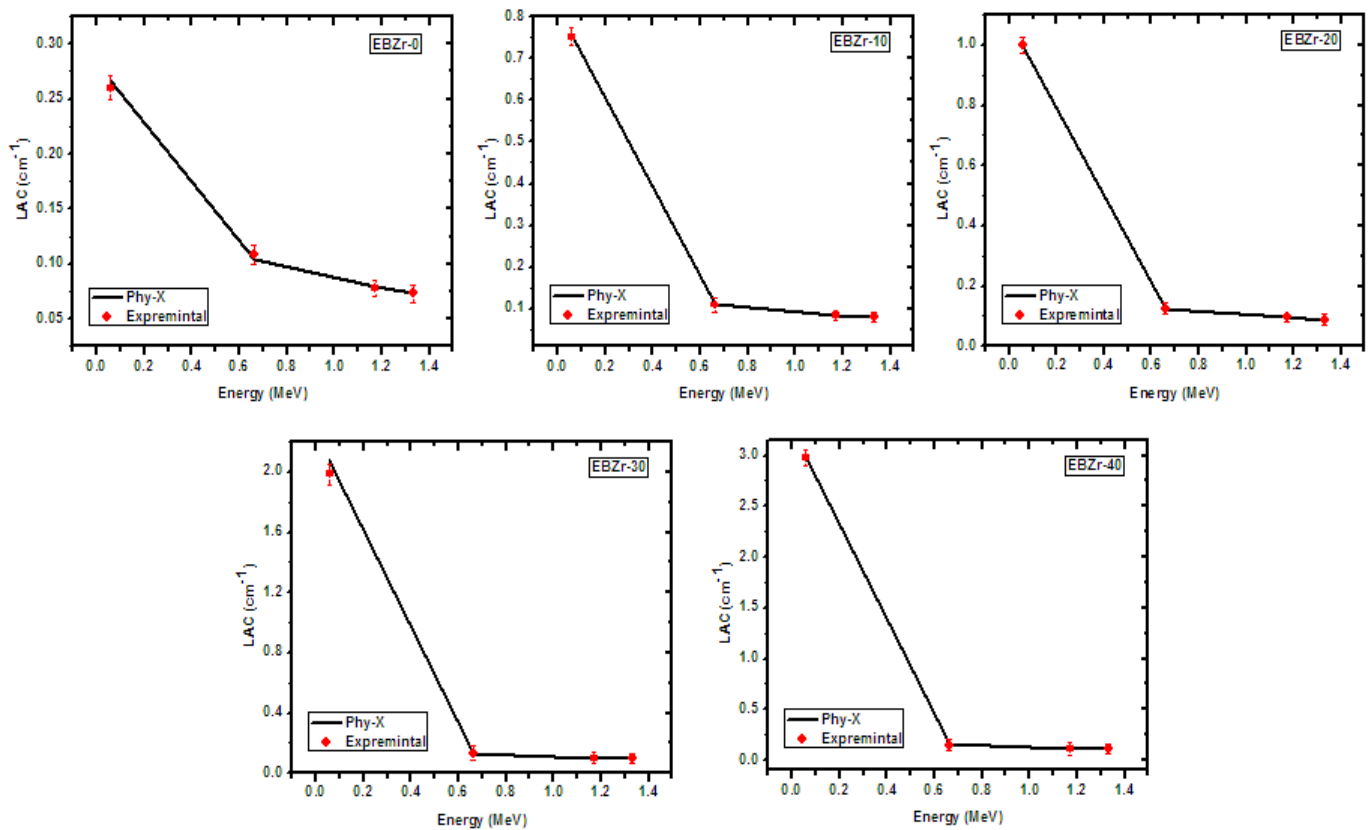


**Figure 3.** Comparison between the experimental and Phy-X linear attenuation coefficients for the new epoxy composites.

We plotted the LACs as a function of ZrO<sub>2</sub> content in Figure 4. The lowest LAC values were reported for EBZr-0 (free of ZrO<sub>2</sub>), and this can be explained according to the low Z atomic content of this sample. It was found that the photon attenuation competence of the present epoxy improved with increasing ZrO<sub>2</sub> content. As is known, high LAC values are a good indicator of superior radiation attenuation competence. Thus we can conclude from Figure 2 that BZr-40 is the best shield among our prepared epoxy samples due to the high LAC for this sample. Additionally, BZr-30 exhibited greater radiation shielding competence than samples BZr-0 to BZr-20, providing confirmation that the addition of ZrO<sub>2</sub> to epoxy has a significant impact on the photon shielding features of the resulting epoxy composite. Quantitatively, the epoxy without ZrO<sub>2</sub> had a LAC of 0.259 cm<sup>-1</sup> at 0.06 MeV, which quickly increased to 2.978 cm<sup>-1</sup> when 40% ZrO<sub>2</sub> was added. For these two epoxy samples, the LACs were, respectively, 0.109 and 0.146 cm<sup>-1</sup> at 0.662 MeV. Thus, it is also to be noted that ZrO<sub>2</sub> has a positive impact on the LAC at 0.06 MeV, which makes these epoxy samples more suitable for applications that require low energy radiation.

As was reported by Kathem et al., pure epoxy and an epoxy/15% wt. Fe<sub>3</sub>O<sub>4</sub> nanocomposite have LAC values of 0.0869 and 0.0971 cm<sup>-1</sup>, respectively (this is at 0.662 MeV) [36]. When this is compared with the LACs of the EBZr-0 to EBZr-40 samples, all of these samples have higher LAC values (0.108, 0.109, 0.124, 0.133, and 0.146 cm<sup>-1</sup>) than those of pure epoxy and the epoxy/15% wt. Fe<sub>3</sub>O<sub>4</sub> nanocomposite. Additionally, Sahin et al. have reported that pure epoxy and epoxy with 30% Yahyali Stone had respective LACs of 0.080 and 0.111 cm<sup>-1</sup> [37]. According to these values, we concluded that the EBZr-20, EBZr-30, and EBZr-40 epoxy composites have better photon shielding competence than the epoxy with 30% Yahyali Stone mentioned above.

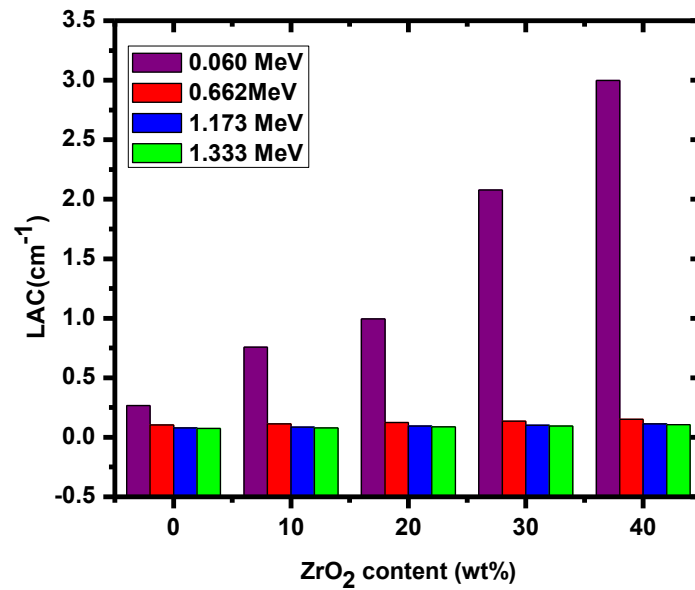


Figure 4. The variation of the LAC values of epoxy with ZrO<sub>2</sub>.

The photon shielding competences of these new epoxy composites (EBZr-0 to EBZr-40) were examined in the context of characteristics called HVL and MFP. The changes of the HVL of the new epoxy composites as determined by experiment are graphed in Figure 5. It is to be noted that the HVL lengths of the epoxy composites reduce with the addition of ZrO<sub>2</sub> for the four selected energies. This implies that introducing ZrO<sub>2</sub> improves the radiation absorption abilities of the epoxy composites due to the high amount of ZrO<sub>2</sub>, which causes an increase in the density of these composites. At 0.06 MeV, the HVL for the ZrO<sub>2</sub>-free epoxy was 2.60 cm, which fell to 0.92 cm following the introduction of 10% ZrO<sub>2</sub>, to 0.70 cm following the introduction of 20% ZrO<sub>2</sub>, to 0.33 following the introduction of 30% ZrO<sub>2</sub>, and to 0.23 cm following the introduction of 40% ZrO<sub>2</sub>. Thus, the HVL at 0.06 MeV decreased from 2.60 to 0.23 cm due to the addition of 40% ZrO<sub>2</sub> to these epoxy composites. When we examined the HVL values at 0.662 MeV, we found that the HVL fell from 6.69 cm to 4.58 cm following the addition of 40% ZrO<sub>2</sub> to these epoxy composites, while it decreased from 8.79 cm to 6.10 cm at 1.173 MeV when the ZrO<sub>2</sub> content was increased from 0% to 40%. These values confirm that the HVL values decrease as the ZrO<sub>2</sub> content level increases in these new epoxy composites.

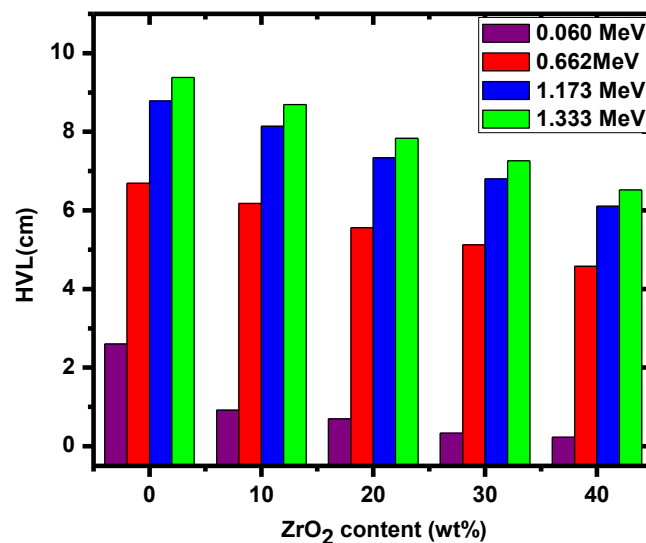


Figure 5. The variation of the half value layer values of epoxy with ZrO<sub>2</sub>.



On the other hand, it was reported by El-Khatib et al. that the HDPE/10 wt% nano CdO has an HVL of 9.36 cm at 1.333 MeV, while Sahin et al. reported an HVL of 8.913 cm for epoxy/30% Yahyali Stone. For our new epoxy composites, the HVL values at 1.333 MeV were 9.38 cm, 8.69 cm, 7.84 cm, 7.27 cm, and 6.52 cm for EBZr-0, EBZr-10, EBZr-20, EBZr-30, and EBZr-40, respectively. Hence, EBZr-20, EBZr-30, and EBZr-40 have lower HVL values than HDPE/10 wt% nano CdO and epoxy/30% Yahyali Stone [38–40].

The variations of the MFP values of the new epoxy composites as determined by experiment are graphed in Figure 6. The MFP values for the five newly developed composites showed the same tendencies as the HVL values. In the other words, as we reported for the HVL values, the MFP values decreased with the introduction of ZrO<sub>2</sub> into these composites. The MFP was relatively high for EBZr-0 (between 3.75 cm and 13.53 cm), while the MFP for EBZr-40 lay within the range of 0.33 cm and 9.41 cm. The difference in the MFP values for the same composite was due to the dependence of the MFP on the energy level. At low energy, the MFP is small, while it increases with increasing energy. The MFP values for these composites were less than 1 cm at 0.06 MeV (standard for EBZr-0), while it was 1.32 cm for EBZr-10. For the other energies, it was higher than 6 cm, and it increased to more than 10 cm for the last energy for all the composites.

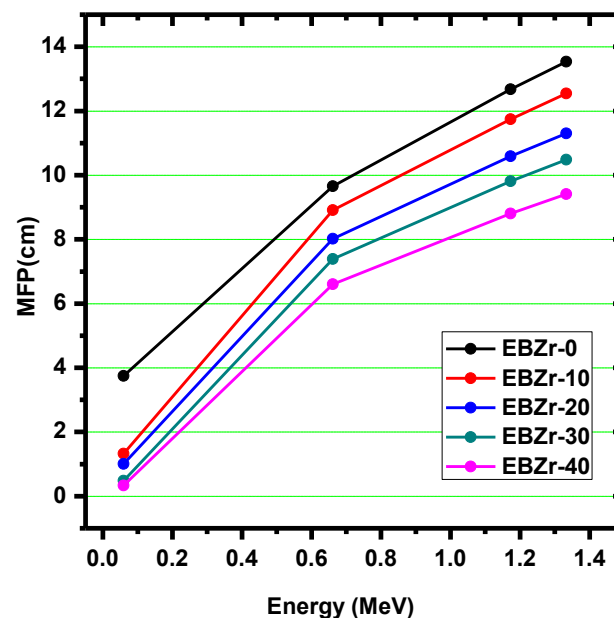


Figure 6. The variation of the mean free path values of epoxy with ZrO<sub>2</sub>.

For the current epoxy composites, the interactions between the radiation and the composites was examined in the context of the radiation absorption ratio (RAR). In Figure 7, we plotted the RAR variation of the pure epoxy and the epoxy with 10–40% ZrO<sub>2</sub>. This is an important parameter since if the value of the RAR for a certain shield is higher than 50%, then this shield can attenuate half of the incoming radiation, while if it is close to 100%, then this shield has interesting shielding abilities and can stop almost all the incoming radiation. Hence, radiation shielding material investigators aim to develop new materials with high RARs (higher than 50%). Taking this fact into consideration, we examined Figure 7 and found that at 0.06 MeV, the RAR for the epoxy composites with ZrO<sub>2</sub> had high RAR values (higher than 50%). For the two composites with 30% and 40% ZrO<sub>2</sub>, the RAR was almost 100% (98.43% and 99.75%, respectively). This means that these two composites are good choices for low energy shielding applications. When the energy increased, the RARs fell to less than 50%. However, we found that higher RAR values improved the attenuation tendencies of these composites. These RAR values are presented for samples with a thickness of 2 cm, but we can improve the RAR for these composites, especially for high energy radiation, by increase the thickness of the composite.

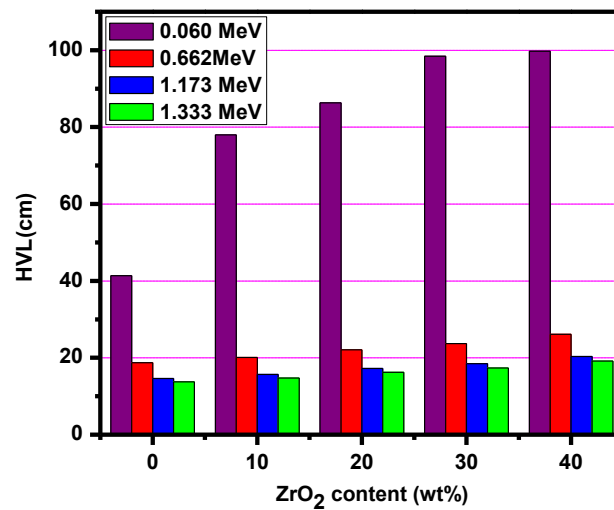


Figure 7. The variation of the radiation absorption ratios of epoxy with ZrO<sub>2</sub>.

The effective atomic number ( $Z_{\text{eff}}$ ) of the epoxy composites were computed using Phy-X software. For the  $Z_{\text{eff}}$  values, we not only selected the four energies used in the previous figures, but we extend the energy range up to 15 MeV. The variations of the  $Z_{\text{eff}}$  values of the epoxy composites without ZrO<sub>2</sub> and with ZrO<sub>2</sub> was determined using Phy-X software, and these have been graphed in Figure 8. The general trend of the  $Z_{\text{eff}}$  values versus the energy is the same for each of the epoxy composites. The  $Z_{\text{eff}}$  values show increased behavior between 0.015 MeV and 0.02 MeV (standard for EBZr-0), and this is due to the K-absorption edge for Zr which occurs at 0.018 MeV, and because EBZr-0 is ZrO<sub>2</sub>-free, so we didn't observe this increase in the  $Z_{\text{eff}}$  trend between 0.015 MeV and 0.02 MeV. Between 0.02 MeV and 0.3 MeV, the  $Z_{\text{eff}}$  values decreased, and the rate of this decrease was very fast. For EBZr-10, the  $Z_{\text{eff}}$  in this interval varied between 27.15 and 4.75, while it is varied between 29.07 and 4.67 for EBZr-20. Above 0.3 MeV and up to around 5 MeV, the  $Z_{\text{eff}}$  values remained constant for all epoxy composites regardless of their ZrO<sub>2</sub> content. Moreover, as the ZrO<sub>2</sub> content increased in the epoxy composites, the  $Z_{\text{eff}}$  values also progressively increased. This increase in the  $Z_{\text{eff}}$  values may be associated with the increase in the weight percentage of high Z-elements (i.e., Zr with atomic number of 40). Thus, we found significant differences in the  $Z_{\text{eff}}$  values between the EBZr-0 and EBZr-40 composites. Quantitatively, the  $Z_{\text{eff}}$  values for these composites were, respectively, 8.66 and 39.70 at 0.02 MeV, 4.74 and 25.00 at 0.06 MeV, 4.27 and 8.22 at 0.2 MeV, and 4.25 and 6.57 at 0.6 MeV.

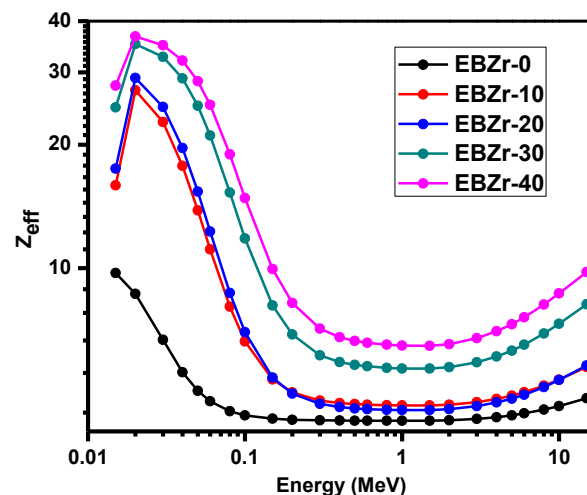


Figure 8. The variation of the effective atomic numbers of epoxy with ZrO<sub>2</sub>.



#### 4. Conclusions

The current work concerns the fabrication of a new, cheap, natural, and ecofriendly radiation shielding composite composed of epoxy containing different quantities of  $ZrO_2$ . To this end, composites EBZr-0 to EBZr-40, which contained 0% to 40%  $ZrO_2$ , were successfully prepared, and we tested their photon shielding competences experimentally, as well as theoretically using Phy-X software, against 0.06, 0.662, 1.173, and 1.333 MeV photons. The shielding abilities of the prepared composites were investigated in the context of the LAC, HVL, RAR, and  $Z_{eff}$  values. All of these parameters demonstrated that  $ZrO_2$  has the potential to improve the radiation protection competences newly developed epoxy composites, since the LAC and  $Z_{eff}$  values increased progressively with increasing  $ZrO_2$  content, while both the HVL and MFP values showed a notable decline with increasing  $ZrO_2$  content. The RAR values for the epoxy composites with  $ZrO_2$  were high at 0.06 MeV (higher than 50%). At this energy, the RAR values for EBZr-30 and EBZr-40 were almost 100% (98.43% and 99.75%, respectively). Hence, these two composites are good choices for low energy shielding applications.

**Author Contributions:** Conceptualization, M.E. and M.I.S.; methodology, N.A.; software, M.A.; validation, F.I.A., A.R.A. and M.E.; formal analysis, N.A.; investigation, M.I.S.; resources, M.A.; data curation, F.I.A.; writing—original draft preparation, M.E.; writing—review and editing, M.I.S.; visualization, F.I.A.; supervision, M.E.; project administration, A.R.A.; funding acquisition, N.A. All authors have read and agreed to the published version of the manuscript.

**Funding:** This research was funded by Princess Nourah bint Abdulrahman University Researchers Supporting Project (PNURSP2022R111), Princess Nourah bint Abdulrahman University, Riyadh, Saudi Arabia.

**Data Availability Statement:** Not applicable.

**Acknowledgments:** This research was funded by Princess Nourah bint Abdulrahman University Researchers Supporting Project (PNURSP2022R111), Princess Nourah bint Abdulrahman University, Riyadh, Saudi Arabia.

**Conflicts of Interest:** The authors declare no conflict of interest.

#### References

1. Aygün, B. High alloyed new stainless steel shielding material for gamma and fast neutron radiation. *Nucl. Eng. Technol.* **2020**, *52*, 647–653. [[CrossRef](#)]
2. Aygün, B. Neutron and gamma radiation shielding Ni based new type super alloys development and production by Monte Carlo Simulation technique. *Radiat. Phys. Chem.* **2021**, *188*, 109630. [[CrossRef](#)]
3. Al-Hadeethi, Y.; Sayyed, M.I. BaO–Li<sub>2</sub>O–B<sub>2</sub>O<sub>3</sub> glass systems: Potential utilization in gamma radiation protection. *Prog. Nucl. Energy* **2020**, *129*, 103511. [[CrossRef](#)]
4. Kamislioglu, M. Research on the effects of bismuth borate glass system on nuclear radiation shielding parameters. *Result Phys.* **2021**, *22*, 103844. [[CrossRef](#)]
5. Tijani, S.A.; Al-Hadeethi, Y. The use of isophthalic-bismuth polymer composites as radiation shielding barriers in nuclear medicine. *Mater. Res. Express* **2019**, *6*, 055323. [[CrossRef](#)]
6. Issa, S.A.M.; Sayyed, M.I.; Zaid, M.H.M.; Matori, K.A. Photon parameters for gamma-rays sensing properties of some oxide of Lanthanides. *Results Phys.* **2018**, *9*, 206–210. [[CrossRef](#)]
7. Tijani, S.A.; Al-Hadeethi, Y.; Sambo, I.; Balogun, F.A. Shielding of beta and bremsstrahlung radiation with transparent Bi<sub>2</sub>O<sub>3</sub>-B<sub>2</sub>O<sub>3</sub>-TeO<sub>2</sub> glasses in therapeutic nuclear medicine. *J. Radiol. Prot.* **2018**, *38*, N44–N51. [[CrossRef](#)]
8. Kaewjaeng, S.; Chanthima, N.; Thongdang, J.; Reungsri, S.; Kothan, S.; Kaewkhao, J. Synthesis and radiation properties of Li<sub>2</sub>O-BaO-Bi<sub>2</sub>O<sub>3</sub>-P<sub>2</sub>O<sub>5</sub> glasses. *Mater. Today Proc.* **2021**, *43*, 2544–2553. [[CrossRef](#)]
9. Chanthima, N.; Kaewkhao, J.; Limkitjaroenporn, P.; Tuscharoen, S.; Kothan, S.; Tungjai, M.; Kaewjaeng, S.; Sarachai, S.; Limsuwan, P. Development of BaO–ZnO–B<sub>2</sub>O<sub>3</sub> glasses as a radiation shielding material. *Radiat. Phys. Chem.* **2017**, *137*, 72–77. [[CrossRef](#)]
10. Alsaiif, N.A.M.; Alotiby, M.; Hanfi, M.Y.; Sayyed, M.I.; Mahmoud, K.A.; Alotaibi, B.M.; Alyousef, H.A.; Al-Hadeethi, Y. A comprehensive study on the optical, mechanical, and radiation shielding properties of the TeO<sub>2</sub>–Li<sub>2</sub>O–GeO<sub>2</sub> glass system. *J. Mater. Sci. Mater. Electron.* **2021**, *32*, 15226–15241. [[CrossRef](#)]
11. Gökç, H.S.; Canbaz-Öztürk, B.; Çam, N.F.; Andıç-Çakır, Ö. Gamma-ray attenuation coefficients and transmission thickness of high consistency heavyweight concrete containing mineral admixture. *Cem. Concr. Compos.* **2018**, *92*, 56–69. [[CrossRef](#)]

12. Gökçe, H.S.; Yalçınkaya, Ç.; Tuyan, M. Optimization of reactive powder concrete by means of barite aggregate for neutrons and gamma rays. *Constr. Build. Mater.* **2018**, *189*, 470–477. [[CrossRef](#)]
13. Obaid, S.S.; Sayyed, M.I.; Gaikwad, D.K.; Pawar, P.P. Attenuation coefficients and exposure buildup factor of some rocks for gamma ray shielding applications. *Radiat. Phys. Chem.* **2018**, *148*, 86–94. [[CrossRef](#)]
14. Sivanesan, D.; Kim, S.; Jang, T.W.; Kim, H.J.; Song, J.; Seo, B.; Lim, C.; Kim, H. Effects of flexible and rigid parts of  $\epsilon$ -caprolactone and tricyclodecanediol derived polyurethane on the polymer properties of epoxy resin. *Polymers* **2021**, *237*, 124374. [[CrossRef](#)]
15. de Kruijff, G.H.M.; Goschler, T.; Beiser, N.; Stenglein, A.; Türk, O.M.; Waldvogel, S.R. Sustainable access to biobased biphenol epoxy resins by electrochemical dehydrogenative dimerization of eugenol. *Green Chem.* **2019**, *21*, 4815–4823. [[CrossRef](#)]
16. Fila, K.; Gargol, M.; Goliszek, M.; Podko'scielna, B. Synthesis of epoxy resins derivatives of naphthalene-2,7-diol and their cross-linked products. *J. Therm. Anal. Calorim.* **2019**, *138*, 4349–4358. [[CrossRef](#)]
17. Higuchi, C.; Horvath, D.; Marcou, G.; Yoshizawa, K.; Varnek, A. Prediction of the glass-transition temperatures of linear Homo/heteropolymers and cross-linked epoxy resins. *ACS Appl. Polym. Mater.* **2019**, *1*, 1430–1442. [[CrossRef](#)]
18. Al-Hadeethi, Y.; Sayyed, M.I.; Barasheed, A.Z.; Ahmed, M.; Elsafi, M. Fabrication of Lead Free Borate Glasses Modified by Bismuth Oxide for Gamma Ray Protection Applications. *Materials* **2022**, *15*, 789. [[CrossRef](#)]
19. Chang, L.; Zhang, Y.; Liu, Y.; Fang, J.; Luan, W.; Yang, X.; Zhang, W. Preparation and characterization of tungsten/epoxy composites for c-rays radiation shielding. *Nucl. Instrum. Methods Phys. Res. B* **2015**, *356–357*, 88–93. [[CrossRef](#)]
20. Kavanoz, H.B.; Akçalı, Ö.; Tokar, O.; Bilmez, B.; Çağlar, M.; İçelli, O. A novel comprehensive utilization of vanadium slag/epoxy resin/antimony trioxide ternary composite as gamma ray shielding material by MCNP 6.2 and BXCOSY. *Radiat. Phys. Chem.* **2019**, *165*, 108446. [[CrossRef](#)]
21. Sevinç, A.H.; Durgun, M.Y. A novel epoxy-based composite with eggshell, PVC sawdust, wood sawdust and vermiculite: An investigation on radiation absorption and various engineering properties. *Constr. Build. Mater.* **2021**, *300*, 123985. [[CrossRef](#)]
22. Aldhuhaibat, M.J.R.; Amana, M.S.; Jubier, N.J.; Salim, A.A. Improved gamma radiation shielding traits of epoxy composites: Evaluation of mass attenuation coefficient, effective atomic and electron number. *Radiat. Phys. Chem.* **2021**, *179*, 109183. [[CrossRef](#)]
23. Saiyad, M.; Devashrayee, N.M. Lifetime estimation of epoxy based composite materials on irradiating with gamma radiation for shielding applications. *Polym. Test.* **2021**, *93*, 106929. [[CrossRef](#)]
24. Zhang, T.; Li, Y.; Yuan, Y.; Cui, K.; Wei, W.; Wu, J.; Qin, W.; Wu, X. Spatially confined  $\text{Bi}_2\text{O}_3\text{-Ti}_3\text{C}_2\text{T}_x$  hybrids reinforced epoxy composites for gamma radiation shielding. *Compos. Commun.* **2022**, *34*, 101252. [[CrossRef](#)]
25. Sayyed, M.I.; Elsafi, M.; Almuqrin, A.H.; Cornish, K.; Elkhatib, A.M. Novel Shielding Mortars for Radiation Source Transportation and Storage. *Sustainability* **2022**, *14*, 1248. [[CrossRef](#)]
26. Sayyed, M.I.; Hamad, M.K.; Mhareb, M.H.A.; Kurtulus, R.; Dwaikat, N.; Saleh, M.; Elsafi, M.; Taki, M.M.; Kavas, T.; Ziq, K.A.; et al. Assessment of radiation attenuation properties for novel alloys: An experimental approach. *Radiat. Phys. Chem.* **2022**, *110152*, in press.
27. Almuqrin, A.H.; Sayyed, M.I.; Elsafi, M.; Khandaker, M.U. Comparison of radiation shielding ability of  $\text{Bi}_2\text{O}_3$  micro and nanoparticles for radiation shields. *Radiat. Phys. Chem.* **2022**, *110170*, in press.
28. Aloraini, D.A.; Sayyed, M.I.; Mahmoud, K.A.; Almuqrin, A.A.H.; Kumar, A.; Khandaker, M.U.; Elsafi, M. Evaluation of radiation shielding characteristics of  $\text{B}_2\text{O}_3\text{-K}_2\text{O-Li}_2\text{O-HMO}$  ( $\text{HMO} = \text{TeO}_2 / \text{SrO} / \text{PbO} / \text{Bi}_2\text{O}_3$ ) glass system: A simulation study using MCNP5 code. *Radiat. Phys. Chem.* **2022**, *110172*, in press. [[CrossRef](#)]
29. Al-Harbi, N.; Sayyed, M.I.; Al-Hadeethi, Y.; Kumar, A.; Elsafi, M.; Mahmoud, K.A.; Khandaker, M.U.; Bradley, D.A. A novel  $\text{CaO-K}_2\text{O-Na}_2\text{O-P}_2\text{O}_5$  glass systems for radiation shielding applications. *Radiat. Phys. Chem.* **2021**, *188*, 109645. [[CrossRef](#)]
30. D'Souza, A.N.; Sayyed, M.I.; Karunakara, N.; Al-Ghamdi, H.; Almuqrin, A.H.; Elsafi, M.; Khandaker, M.U.; Kamath, S.D.  $\text{TeO}_2\text{-SiO}_2\text{-B}_2\text{O}_3$  glasses doped with  $\text{CeO}_2$  for gamma radiation shielding and dosimetry application. *Radiat. Phys. Chem.* **2022**, *110233*, in press.
31. Sayyed, M.I.; Alrashedi, M.F.; Almuqrin, A.H.; Elsafi, M. Recycling and optimizing waste lab glass with  $\text{Bi}_2\text{O}_3$  nanoparticles to use as a transparent shield for photons. *J. Mater. Res. Technol.* **2022**, *17*, 2073–2083. [[CrossRef](#)]
32. Al-Hadeethi, Y.; Sayyed, M.I.; Barasheed, A.Z.; Ahmed, M.; Elsafi, M. Preparation and radiation attenuation properties of ceramic ball clay enhanced with micro and nano ZnO particles. *J. Mater. Res. Technol.* **2022**, *17*, 223–233. [[CrossRef](#)]
33. Hannachi, E.; Sayyed, M.I.; Slimani, Y.; Elsafi, M. Experimental investigation on the physical properties and radiation shielding efficiency of  $\text{YBa}_2\text{Cu}_3\text{O}_y / \text{M@M}_3\text{O}_4$  ( $\text{M} = \text{Co}, \text{Mn}$ ) ceramic composites. *J. Alloys Compd.* **2022**, *904*, 164056. [[CrossRef](#)]
34. Hannachi, E.; Sayyed, M.I.; Slimani, Y.; Almessiere, M.A.; Baykal, A.; Elsafi, M. Synthesis, characterization, and performance assessment of new composite ceramics towards radiation shielding applications. *J. Alloys Compd.* **2022**, *899*, 163173. [[CrossRef](#)]
35. Elsafi, M.; Koraim, Y.; Almurayshid, M.; Almasoud, F.I.; Sayyed, M.I.; Saleh, I.H. Investigation of Photon Radiation Attenuation Capability of Different Clay Materials. *Materials* **2021**, *14*, 6702. [[CrossRef](#)] [[PubMed](#)]
36. Kathem, H.O.; Resen, M.J.; Jubier, N.J. Characterization of radiation attenuation properties of 0.662 MeV gamma ray energy for epoxy  $\text{Fe}_3\text{O}_4$  composite shields. *Indian J. Nat. Sci.* **2018**, *9*, 14609–14615.
37. El-Nahal, M.A.; Elsafi, M.; Sayyed, M.I.; Khandaker, M.U.; Osman, H.; Elesawy, B.H.; Saleh, I.H.; Abbas, M.I. Understanding the Effect of Introducing Micro- and Nanoparticle Bismuth Oxide ( $\text{Bi}_2\text{O}_3$ ) on the Gamma Ray Shielding Performance of Novel Concrete. *Materials* **2021**, *14*, 6487. [[CrossRef](#)]
38. El-Khatib, A.M.; Abbas, M.I.; Elzaher, M.A.; Badawi, M.S.; Alabsy, M.T.; Alharshan, G.A.; Aloraini, D.A. Gamma attenuation coefficients of nano cadmium oxide/high density polyethylene. *Compos. Sci. Rep.* **2019**, *9*, 16012. [[CrossRef](#)]

39. Sahin, N.; Bozkurt, M.; Karabul, Y.; Kılıç, M.; Ozdemir, Z.G. Low cost radiation shielding material for low energy radiation applications: Epoxy/Yahyali Stone composites. *Prog. Nucl. Energy* **2021**, *135*, 103703. [[CrossRef](#)]
40. Şakar, E.; Özpolat, Ö.F.; Alım, B.; Sayyed, M.I.; Kurudirek, M. Phy-X/PSD: Development of a user friendly online software for calculation of parameters relevant to radiation shielding and dosimetry. *Radiat. Phys. Chem.* **2020**, *166*, 108496. [[CrossRef](#)]